0013-7227/06/$15.00/0
Printed in U.S.A.

Endocrinology 147(10):4781–4791

doi: 10.1210/en.2006-0544

Pituitary Tumor Transforming Gene Overexpression Facilitates Pituitary Tumor Development

Ines Donangelo, Shiri Gutman, Eva Horvath, Kalman Kovacs, Kolja Wawrowsky, Michael Mount, and Shlomo Melmed

Department of Medicine (I.D., S.G., K.W., M.M., S.M.), Cedars-Sinai Research Institute, David Geffen School of Medicine at University of California Los Angeles, Los Angeles, California 90048; and St. Michael's Hospital (E.H., K.K.), Toronto, Ontario, Canada M5B 1W8

Intrinsic and extrinsic stimuli result in profound pituitary growth changes ranging from hypoplasia to hyperplasia. Pituitary tumor transforming gene (PTTG) abundance correlates with pituitary trophic status. Mice with *Pttg* inactivation exhibit pituitary hypoplasia, whereas targeted pituitary *PTTG* overexpression driven by α-subunit glycoprotein (αGSU) promoter results in focal pituitary hyperplasia. To test the impact of pituitary hyperplasia on tumor development, we crossbred *αGSU.PTTG* with *Rb*+/− mice, which develop pituitary tumors with high penetrance. Pituitary glands of resulting bitransgenic *αGSU.PTTGxRb*+/− mice were compared with monotransgenic *αGSU.PTTG*, *Rb*+/−, and wild-type mice. Confocal microscopy showed that *PTTG*-overexpressing cells have enlarged nuclei and marked redistribution of chromatin, and electron microscopy of *αGSU.PTTG* pituitaries showed enlarged gonadotrophs with prominent Golgi complexes and numerous secretory granules. These morphological findings were even more remarkable in *αGSU.PTTGxRb*+/− pituitaries. Mice from all four genotypes were sequentially imaged by magnetic resonance imaging to evaluate pituitary volume, and glands from *αGSU.PTTGxRb*+/− mice were the largest as early as 2 months of age ($P = 0.0003$). Cumulative incidence of pituitary tumors visualized by magnetic resonance imaging did not differ between *Rb*+/− and *αGSU.PTTGxRb*+/− mice. However, anterior lobe tumors determined after necropsy were 3.5 times more frequent in *αGSU.PTTGxRb*+/− than in *Rb*+/− mice ($P = 0.0036$), whereas the frequency of intermediate lobe tumors was similar. In summary, *αGSU.PTTGxRb*+/− pituitary glands exhibit enhanced cellular activity, increased volume, and higher prevalence of anterior pituitary tumors, indicating that changes in pituitary PTTG content directly relate to both pituitary trophic status and tumorigenic potential. (*Endocrinology* 147: 4781–4791, 2006)

DESPITE ADVANCES IN understanding the pathogenesis of pituitary tumors, the primary etiology of these common adenomas remains enigmatic. Pituitary tumor formation and progression occurs in a relatively diverse background of chromosomal instability, epigenetic changes, and cell mutations (1–3). Compared with the normal pituitary gland, a wide range of gene expression profiles is observed between the different pituitary adenomas subtypes (4, 5). With the exception of the Gsα mutation found in approximately one third of GH-secreting adenomas (6–9), there are few clearly defined proximal pathways for human pituitary tumorigenesis.

Extrinsic and intrinsic signals subserve remarkable pituitary gland plasticity, with changes in pituitary size ranging from hypoplasia to hyperplasia (10). In animal models, pituitary trophic status correlates with the likelihood of tumor development because hyperplastic pituitary glands frequently develop adenomas, suggesting that sustained long-term pituitary hyperplasia ultimately results in tumor formation (11, 12). At the opposite end of the spectrum, hypoplasia likely protects the pituitary from tumor development. In mouse models with combined hypoplastic and tumorigenic genetic abnormalities, tumor incidence is lower than in mice harboring the tumorigenic genetic change alone. This pattern is observed in both *Pttg*−/−*Rb*+/− mice (inactivation of *pttg* leads to pituitary hypoplasia, and *Rb* disruption causes pituitary tumor) and in double-mutant *p18Ink4c*−/−*cdk4*−/− mice (p18 inactivation causes pituitary hyperplasia that progresses to tumor, and loss of cdk4 results in pituitary hypoplasia) (13, 14). Understanding mechanisms that regulate pituitary plasticity therefore provides insights for disrupting development and progression of pituitary tumors.

Pituitary tumor transforming gene (*PTTG*) was isolated from a pituitary tumor cell line, and its overexpression results in cellular transformation *in vitro* and tumor formation in nude mice (15). PTTG was identified as the index mammalian securin, regulating sister chromatid separation during mitosis (16), and excessive or suppressed PTTG levels result in aneuploidy (17, 18). PTTG abundance correlates with pituitary gland plasticity. Transgenic mouse models of both *PTTG* overexpression and inactivation support a causal role for changes in PTTG levels on development of pituitary hyperplasia and hypoplasia and on conferring tumor growth advantage or tumor growth protection, respectively (Table 1). Mice with transgenic expression of human *PTTG1* driven by the α-subunit glycoprotein (αGSU) promoter express *PTTG* in LH-, FSH-, TSH-, and GH-secreting cells (19).

First Published Online June 29, 2006

Abbreviations: eGFP, Enhanced green fluorescent protein; αGSU, α-subunit glycoprotein; MRI, magnetic resonance imaging; PRL, prolactin; PTTG, pituitary tumor transforming gene; RER, rough endoplasmic reticulum; RMANOVA, repeated measures ANOVA; TRITC, tetramethylrhodamine B isothiocyanate; WT, wild type.

***Endocrinology* is published monthly by The Endocrine Society (http://www.endo-society.org), the foremost professional society serving the endocrine community.**

TABLE 1. Pituitary phenotype in murine models of *PTTG* overexpression (*αGSU.PTTG*) or inactivation (*pttg−/−*)

Pituitary phenotype	*αGSU.PTTG* mice	*Pttg−/−* mice
Trophic status	Focal hyperplasia	Diffuse hypoplasia
Tumorigenic potential	Plurihormonal microadenomas	Protective effect, as observed in *Pttg−/−Rb+/−* mice
Hormonal status	Increased serum levels of LH, testosterone, GH, and IGF-I	Not available

αGSU.PTTG mice develop histopathological pituitary findings ranging from frequent hyperplasia to occasional microadenomas. Increased serum LH, testosterone, GH, and IGF-I levels result in marked seminal vesicle and prostate enlargement in male *αGSU.PTTG* mice. In contrast, *Pttg* inactivation results in opposite trophic effects, *i.e.* pituitary, pancreatic β-cell, splenic, and testicular hypoplasia (18).

To further understand the role of *PTTG* on pituitary tumor development, *αGSU.PTTG* mice were crossbred with *Rb+/−* mice, a well-established mouse model for pituitary tumors (20). The pituitary glands of the resulting bitransgenic *αGSU.PTTGxRb+/−* mice exhibited marked hyperplasia and higher prevalence of anterior lobe pituitary tumors, compared with singly transgenic *αGSU.PTTG* or *Rb+/−* mice. These findings indicate that changes in PTTG abundance correlate with pituitary tumorigenic potential.

Materials and Methods

Animals

This study was approved by the Institutional Animal Care and Use Committee and was performed according to the National Institutes of Health Guide for the Care and Use of Laboratory Animals. Mice of a B6C3 genetic background harboring the PαGSU-PTTG1-IRES-eGFP (*αGSU.PTTG*) transgene were previously described (19). *Rb+/−* mice on a 129/Sv genetic background were purchased from The Jackson Laboratory (Bar Harbor, ME) and backcrossed for four generations to a C57BL/6 parental genotype. *αGSU.PTTG* mice were crossbred with *Rb+/−* mice for two generations, resulting in offspring with the following genotypes: wild type (WT), *αGSU.PTTG*, *Rb+/−*, and bitransgenic *αGSU.PTTGxRb+/−*. Animals were genotyped by PCR for the presence of enhanced green fluorescent protein (eGFP) (19) and *Rb* mutation (20) as previously described. Phenotype analysis was performed by comparing litter mates with different genotypes.

Bitransgenic *αGSU.PTTGxRb+/−* mice and age- and sex- matched controls (*αGSU.PTTG*, *Rb+/−*, and WT) were euthanized using CO_2 chambers. Blood was withdrawn directly from the heart, pituitary glands were collected and weighed, and other organs were carefully inspected and collected for analysis if abnormal.

Morphological methods

For light microscopy, the pituitaries were fixed in 10% buffered formalin, paraffin embedded, sectioned 4 microns thick, and stained with hematoxylin and eosin. Sections were also analyzed by double-label immunohistochemistry as previously described (19), using the antibodies: rabbit antihuman ACTH (1:200), rabbit antirat GH (1:800), rabbit antirat TSHβ (1:200), guinea pig antirat prolactin (PRL) (1:200), guinea pig antirat LHβ (1:200), and guinea pig antirat α-subunit (1:200) (National Hormone and Peptide Program, National Institute of Diabetes and Digestive and Kidney Diseases, Bethesda, MD). Secondary antibodies were Alexa Fluor 488 antiguinea pig and Alexa Fluor 568 antirabbit (Molecular Probes, Carlsbad, CA). Slides were counterstained with 4,6-diamidino-2-phenylindole to visualize nuclei.

PCNA nuclear staining was performed according to instructions provided by the kit (Zymed Laboratories, Inc., San Francisco, CA), and index of stained nuclei was determined by a rater (S.G.) blinded for genotype with Image J cell counter (21).

For electron microscopy, small pituitary pieces were fixed in 2.5% glutaraldehyde in 0.1 M sodium cacodylate buffer, postfixed in 1% osmium tetroxide, processed through graded series of ethanol, then propylene oxide, and embedded in Araldite. Semithin sections stained with toluidine blue, and ultrathin sections with uranyl acetate and lead citrate were studied with a Philips 410-LS electron microscope (Phillips Electronic Instruments, Rahway, NJ).

Confocal microscope images were obtained using a TCS-SP confocal scanner (Leica Microsystems, Mannheim, Germany). Before imaging, pituitary samples were fixed in 10% buffered formalin for 2 h and then incubated in 2 μM TO-PRO-3 (Molecular Probes) and 50 μM phalloidin-tetramethylrhodamine B isothiocyanate (TRITC) (Sigma-Aldrich, St. Louis, MO) overnight for nucleic acid and actin filament staining, respectively. A Plan Apo 63 × 1.2 numerical aperture lens was used, and the dimensions of the confocal stacks were 150 × 150 μm and 10–15 μm deep. To excite the fluorescent dyes, three different lasers were used in sequential acquisition mode: 488-nm line of argon laser for eGFP, 568-nm line of argon-krypton laser for phalloidin-TRITC, and 633-nm line of helium-neon laser for TO-PRO-3. Cells expressing αGSU.PTTG were promptly identified due to presence of eGFP signal. Images from different fields of the pituitary were obtained, and analysis of nuclear morphology was performed without knowledge of eGFP status, *i.e.* the green layer of the image was hidden using Adobe Photoshop 5.5 (Adobe Systems, San Jose, CA) software. Nuclei were considered altered if they were clearly different from the average WT pituitary cell (Fig. 1a), *i.e.* if

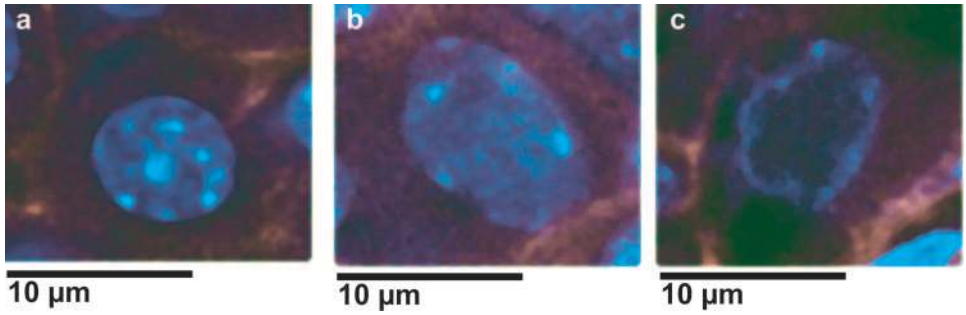

FIG. 1. Confocal microscopy images of pituitary nuclei used as reference for classification into normal or altered morphology. a, Normal-sized nucleus with habitual chromatin distribution, *i.e.* with scattered foci of heterochromatin. b, Unusually enlarged nucleus with very few heterochromatin foci located close to the nuclear membrane. c, Nucleus with altered distribution of chromatin concentrated in the nuclear periphery, forming a ring-shaped pattern. Nucleic acid is stained with TO-PRO-3 (*blue*), and actin filaments were stained with phalloidin-TRITC (*red*) to help define cell boundaries.

the nucleus was markedly enlarged (Fig. 1b) or showed diffuse or peripheral accumulation of nucleic acid (Fig. 1, b and c, respectively) as opposed to the presence of dense and mainly central heterochromatin foci in WT nuclei (Fig. 1a). Nuclei that could not be undoubtedly classified as normal or altered were excluded from evaluation, and this was the case in 14% (35 of 248) of WT, 17% (54 of 314) of αGSU.PTTG, 24% (69 of 291) of Rb+/−, and 24% (61 of 256) of αGSU.PTTGxRb+/− analyzed cells. After classification of nuclear morphology, eGFP status was revealed, and the nuclear morphology profile from cells overexpressing PTTG (eGFP positive) or not (eGFP negative) was contrasted.

Magnetic resonance imaging (MRI)

Pituitary glands were imaged *in vivo* with MRI, as previously described (19), in eight WT, 10 *αGSU.PTTG*, nine *Rb+/−*, and 10 bitransgenic *αGSU.PTTGxRb+/−* mice with similar proportion of males and females, starting at 2 months of age, and then every 2 months until 10 months. Briefly, mice were anesthetized with ip injections of ketamine (70 μg/g) and medetomidine (1 μg/g) and imaged using a small solenoidal receiver coil. Atipamezole (1 μg/g ip) was used to reverse the effect of medetomidine. The pituitary area from each sagittal plane was determined by manually drawing a line along the edge of the gland in a magnified image. Two independent raters (S.G. and M.M.) blinded for mice genotype performed this measurement. Pituitary volume was determined by adding the number of pixels within the pituitary gland of all the sagittal planes.

Statistical analysis

Statistical calculations and significance tests were performed using the statistical software package SAS version 9.1 (SAS Institute, Cary, NC). Reproducibility of pituitary volume measurement by MRI was determined as follows: in nine mice, the pituitary was imaged three consecutive times, repositioning the animals between each imaging. The mean absolute percent difference in pituitary volume between three different images was 5.47, ranging from 0.5–13.7%. Changes of pituitary volume across time were assessed by repeated measures ANOVA (RMANOVA) with time (age) as the within-subjects factor (at four levels: 2, 4, 6, and 8 months) and genotype as the between-subjects factor (at four levels: WT, *Rb+/−*, *αGSU.PTTG*, and *αGSU.PTTGxRb+/−*). Because volumes should be related across time, an autoregressive covariance structure was assumed for the RMANOVA. Genotype differences in mean volume at a specific time were assessed by one-way ANOVA; *post hoc* comparisons were performed by Dunnett's *t* test with WT as the control group. Frequency of intermediate lobe and anterior lobe pituitary tumors in *Rb+/−* and *αGSU.PTTGxRb+/−* mice was compared by Fisher's exact test.

Results

Electron microscopy: PTTG overexpression results in prominent Golgi activity and increase number of secretory granules

Ten pituitaries derived from all the genotypes were analyzed by electron microscopy (3- to 5-month-old males and females). Ultrastructure of cell types in pituitaries derived from *αGSU.PTTG* mice was normal, with the exception of gonadotrophs, as shown in Fig. 2B. These cells were slightly to moderately enlarged and appeared more numerous when compared with WT specimens (Fig. 2A). Gonadotrophs exhibited unusually abundant secretory granules and prominent, very active Golgi complexes (Fig. 2B). Occasional cells not typical of pituitary cell types were encountered; these were large, lucent, and exhibited secretory granules of variable sizes and prominent Golgi complexes, suggesting altered or differentiating gonadotrophs, as shown in Fig. 2C (*arrowhead*).

Electron microscopy of pretumorous pituitary glands derived from *Rb+/−* mice did not show obvious abnormalities.

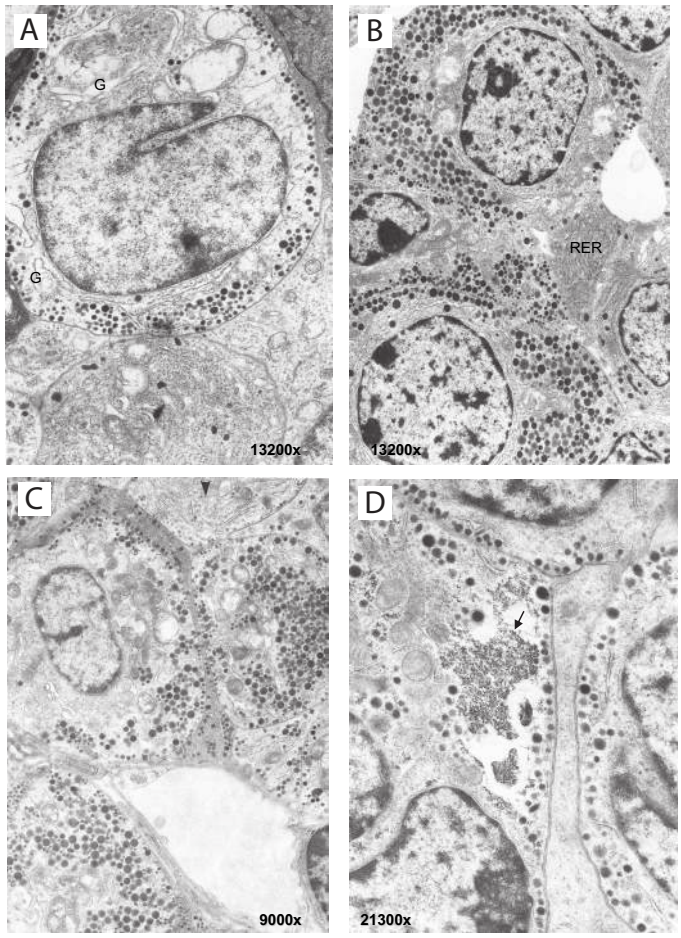

FIG. 2. Electron microscopy images of mice pituitary glands. A, WT specimen depicting a normal gonadotroph cell including populations of small and large secretory granules. Gonadotrophs are ovoid cells that exhibit well-developed RER, ring-shaped Golgi complex, and two different sizes of secretory granules. Part of a PRL cell is shown as well (*bottom*). Magnification, ×13,200. B, Monotransgenic *αGSU.PTTG* pituitary specimen showing portions of three hyperplastic gonadotrophs. The secretory granules are more numerous than usual; the RER is well developed, but not dilated. The other cell type shown is a lactotroph (*right*). Magnification, ×13,200. C, Bitransgenic *αGSU.PTTGxRb+/−* specimen with marked gonadotroph hyperplasia; both small and large secretory granules are abundant, the Golgi complex is prominent, and the RER shows normal morphology. *Top*, Part of an unidentified cell with lucent cytoplasm and minute, sparse, peripherally disposed secretory granules is depicted (*arrowhead*). Magnification, ×9000. D, *αGSU.PTTGxRb+/−* specimen with aggregates of glycogen β particles (*arrow*) not known to normally occur are evident within the cytoplasm of a hyperplastic gonadotroph. Magnification, ×21,300. G, Golgi complex.

A pituitary tumor sample derived from an 11-month-old *Rb+/−* female showed a cell population with low-grade functional differentiation, with numerous small vacuolated rough endoplasmic reticulum (RER) profiles, as well as a well-developed Golgi complex containing occasional immature granules. Light microscopy and immunostaining for pituitary hormones of this tumor sample identified it as an ACTH-positive intermediate lobe tumor (data not shown).

Pituitary glands derived from *αGSU.PTTGxRb+/−* mice exhibited heterogeneous cell morphology, ranging from areas with large, lucent cells with minute secretory granules

(presumably altered or differentiating gonadotrophs) similar to those observed in *αGSU.PTTG* pituitaries (Fig. 2C, *arrowhead*), to massive gonadotroph hyperplasia. The ultrastructural appearance of hyperplastic gonadotroph cells shows several small (150–350 nm) and many larger (over 350 nm) secretory granules, but no proliferation or dilatation of RER (Fig. 2C), the salient feature of so-called castration cells. Notably, glycogen β-particles were present in the cytoplasm of several gonadotrophs (Fig. 2D). In addition, small areas of hyperplastic thyrotroph cells were also noted. These cells are polyhedral or elongated and exhibit well-developed and dilated RER, but without the so-called thyroidectomy changes. Two distinct morphological tumor types were observed in a pituitary derived from a 5-month-old *αGSU.PTTGxRb+/−* male; one tumor subtype was probably of gonadotroph origin (Fig. 3A), whereas the second tumor was likely derived from a thyrotroph cell (Fig. 3B). Pituitary tumors derived from two *αGSU.PTTGxRb+/−* females (12 and 13 months old) were also analyzed. Frank neoplasia likely of gonadotroph origin and areas of gonadotroph and thyrotroph hyperplasia similar to those found in younger *αGSU.PTTGxRb+/−* mice were observed.

Confocal microscopy: PTTG overexpression results in chromatin reorganization

Pituitaries from 2-month-old WT, *Rb+/−*, monotransgenic *αGSU.PTTG*, and bitransgenic *αGSU.PTTGxRb+/−* females from the same litter were imaged with confocal microscopy. A representative confocal image from *αGSU.PTTG* pituitary can be appreciated in Fig. 4, where distinct nuclear morphology from cells overexpressing *PTTG* transgene (eGFP signal) can be promptly contrasted with the normal (eGFP negative) nuclear morphology. Pituitary cells were individually analyzed by studying their whole extent through the several confocal layers. Figure 5 shows representative samples of pituitary cell nuclei observed in the four genotypes, and nuclear morphology analysis is summarized in Table 2. In WT pituitary, 9% (19 of 213) of nuclei were classified as altered. In *Rb+/−* pituitary, the frequency of altered nuclei increased to 28% (62 of 222) mainly due to the presence of nuclei with diffuse chromatin distribution (poorly defined heterochromatin) (Fig. 5, j–n) because macronuclei were seldom observed in this genotype. The cell population in both monotransgenic *αGSU.PTTG* and bitransgenic *αGSU.PTTGxRb+/−* pituitaries was divided into eGFP-negative (normal *Pttg* expression) and eGFP-positive (cells expressing *PTTG* transgene). Within the eGFP-negative cells, the frequency of altered nuclei was 23% (10 of 43) and 14% (13 of 93) in *αGSU.PTTG* and *αGSU.PTTGxRb+/−*, respectively. On the other hand, nuclei in pituitary cells overexpressing *PTTG* (eGFP positive) were generally altered. Eighty-eight percent (192 of 217) of eGFP-positive cells in monotransgenic *αGSU.PTTG* (Fig. 5, f–i) and 95% (97 of 102) of eGFP-positive cells in bitransgenic *αGSU.PTTGxRb+/−* pituitaries (Fig. 5, o–r) exhibited altered nuclei. In addition to large nuclei and redistribution of chromatin, a fraction (~15%) of altered nuclei in bitransgenic *αGSU.PTTGxRb+/−* pituitary glands also exhibited large areas within the nuclei that did not stain with TO-PRO-3 (Fig. 5, o and p).

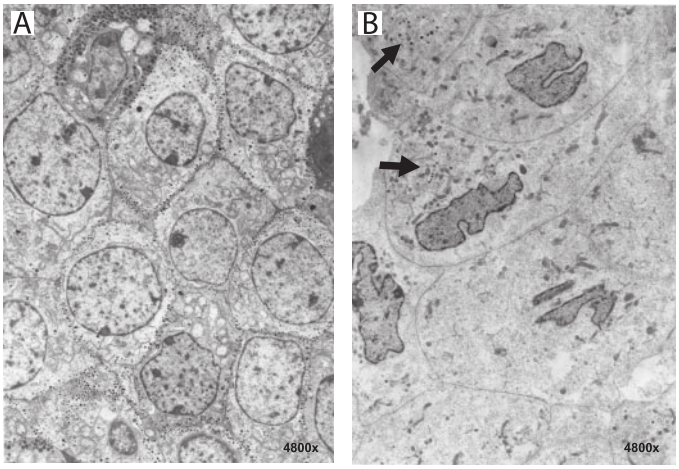

FIG. 3. Ultrastructural appearance of a bitransgenic *αGSU.PTTGxRb+/−* pituitary specimen with two distinct neoplasms. A, one presumably of gonadotroph derivation; features of uniform ovoid nuclei, lucent cytoplasm, paucity of organelles and sparse, minute, peripheral secretory granules resemble those of the unidentified cell type (see Fig. 2C). Magnification, ×4800. B, Second tumor, likely of thyrotroph origin, features large irregular cells with markedly irregular nuclei. The sizable, low-density cytoplasm is loosely filled with vesicular RER, and small secretory granules are noted only within the Golgi region (*arrows*). Magnification, ×4800.

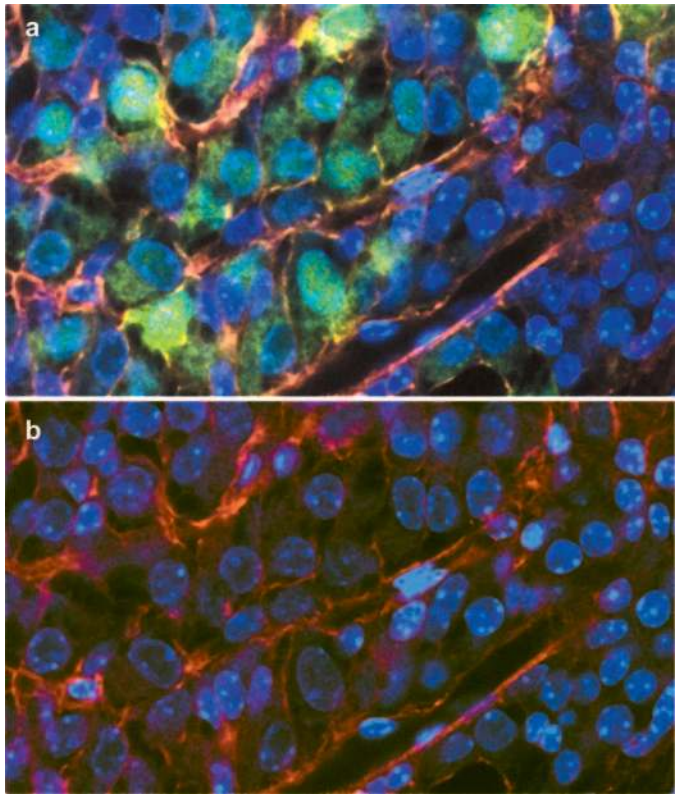

FIG. 4. Overview of pituitary cells expressing *αGSU-PTTG1-IRES-eGFP* transgene. a and b, Duplicates of the same image, where a is the untouched image, and in b, the *green layer* (eGFP) has been hidden for better visualization of nuclear morphology. Contrast between eGFP positive (overexpressing PTTG) and eGFP negative (normal *PTTG* content) can be appreciated, notably presence of macronuclei and reorganization of chromatin.

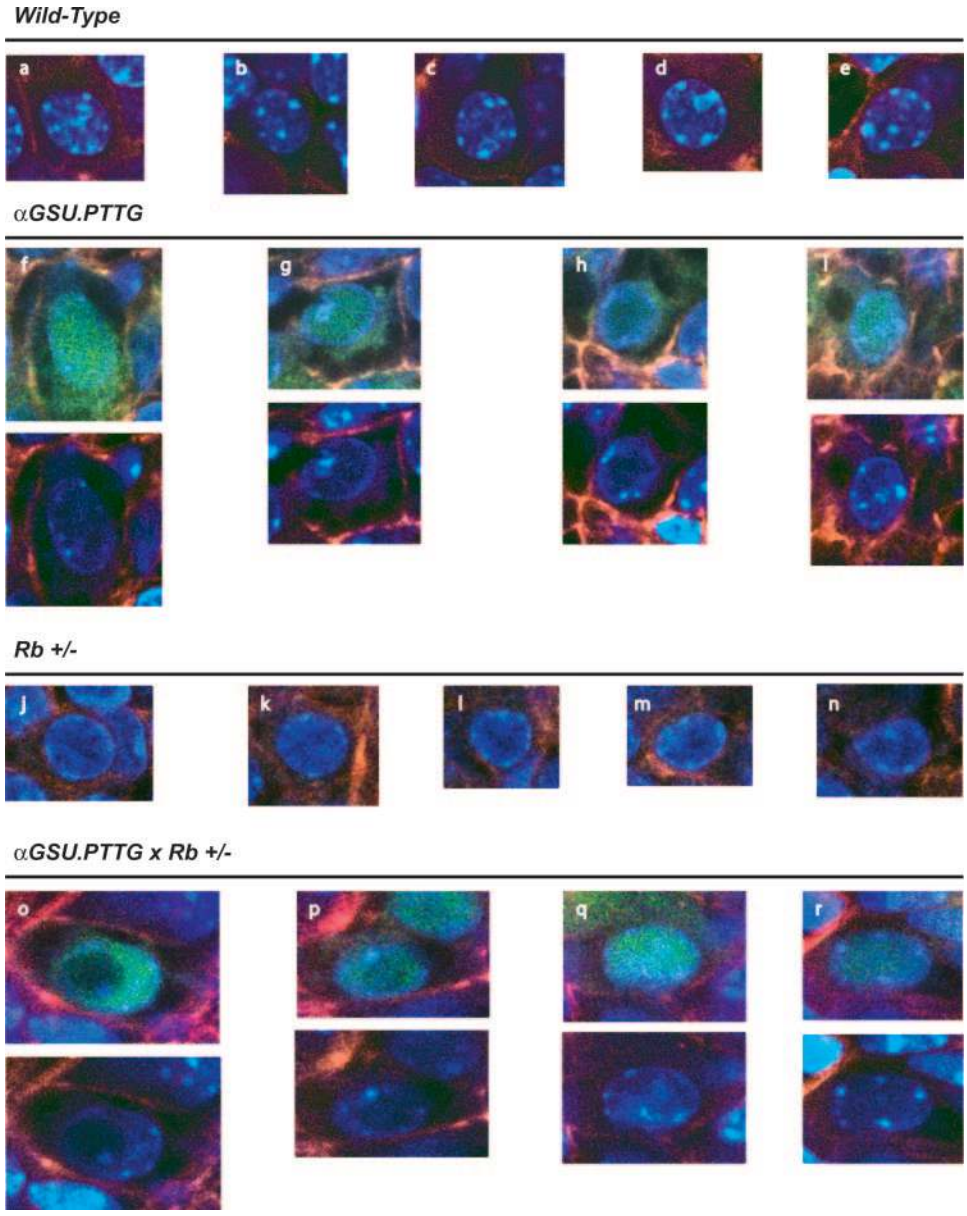

FIG. 5. Confocal microscopy images of cells from WT, monotransgenic *αGSU.PTTG, Rb+/−*, and bitransgenic *αGSU.PTTGxRb+/−* pituitaries. Representative samples of WT (a–e) pituitary cells with oval-shaped nuclei and readily identified foci of condensed chromatin. The transgene expressing *PTTG* is tagged with eGFP; therefore, in *αGSU.PTTG* and *αGSU.PTTGxRb+/−* pituitaries, cells overexpressing *PTTG* were identified by the presence of eGFP (f–i and o–r, *top* images). Upon removal of *green layer* (f–i and o–r, *bottom images*), altered nuclei were visible: macronuclei (f and o–r, *bottom*), redistribution of chromatin, *i.e.* loss of central foci of heterochromatin (f–i and o–r, *bottom*) and accumulation of chromatin adjacent to the nuclear membrane (g–i, *bottom*). In a fraction of *Rb+/−* pituitary cells, heterochromatin foci were not identified (j–n), and this chromatin distribution pattern was considered altered. Nucleic acid is stained with TO-PRO-3 (*blue*) and actin filament with phalloidin-TRITC (*red*).

These large nuclear vacuoles were also noted less frequently in cells from *αGSU.PTTG* pituitary.

αGSU.PTTGxRb+/− mice exhibit marked pituitary enlargement

Pituitary volume was assessed by MRI in bitransgenic *αGSU.PTTGxRb+/−* mice and compared with WT, monotransgenic *αGSU.PTTG*, and *Rb+/−* mice starting at 2 months of age and then every 2 months for 10 months. Volume assessment by this method allowed comparison of pituitary enlargement caused by hyperplasia among the different genotypes and distinguished pituitary growth caused by hyperplasia *vs.* adenoma. To assess information on pretumorous pituitary growth, mice exhibiting tumors visualized by MRI were excluded. The RMANOVA pituitary volume model was highly significant ($P < 0.0001$), and mean pituitary volumes (averaging across time) differed by genotype ($P = 0.016$). As shown in Fig. 6, at 2 months of age, bitransgenic *αGSU.PTTGxRb+/−* mice had increased pituitary volumes compared with WT pituitary volumes (234 ± 39 *vs.* 179 ± 20 pixels, $P = 0.0003$; ANOVA). Bitransgenic *αGSU.PTTGxRb+/−* mice also exhibited the largest pituitary volumes at 4, 6, and 8 months; however, the difference from other genotypes was not significant at these times. The pattern of pituitary growth over time was similar between sexes (data not shown).

Pituitary tumor development assessed by MRI

Distinct pituitary tumors were detected by MRI in *Rb+/−* and bitransgenic *αGSU.PTTGxRb+/−* mice but not in WT or monotransgenic *αGSU.PTTG* mice. Pituitary tumors were identified between 1 and 4 months before animals became visibly ill, allowing follow-up of tumor growth, as depicted in Fig. 7. Cumulative pituitary tumor incidence until age 10

TABLE 2. Nuclear morphology according to genotype and eGFP status

Genotype	Nuclear morphology	
	eGFP negative (%)	eGFP positive (%)
Wild-type		
Altered	19 (9)	
Normal	194 (91)	
Total	213 (100)	
αGSU.PTTG		
Altered	10 (23)	192 (88)
Normal	33 (77)	25 (12)
Total	43 (100)	217 (100)
Rb+/−		
Altered	62 (28)	
Normal	160 (72)	
Total	222 (100)	
αGSU.PTTGxRb+/−		
Altered	13 (14)	97 (95)
Normal	80 (86)	5 (5)
Total	93 (100)	102 (100)

months as assessed by MRI was not different between *Rb+/−* and *αGSU.PTTGxRb+/−* mice (Fig. 8A); however, qualitative differences were noted when comparing tumors from both genotypes. Two mice died before 10 months due to tumor mass, and they were maintained in the cumulative pituitary tumor incidence analysis because their tumors had been detected by MRI.

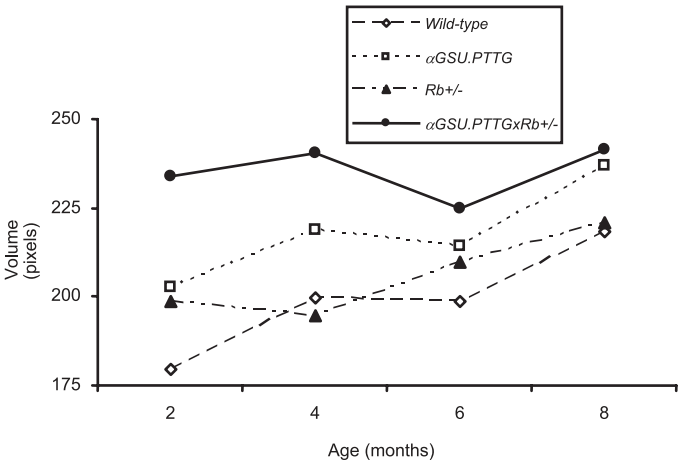

FIG. 6. Bitransgenic *αGSU.PTTGxRb+/−* mice exhibit significantly larger pituitaries across genotypes ($P = 0.016$). Shown are average pituitary gland volumes as assessed by MRI in WT, *αGSU.PTTG, Rb+/−*, and *αGSU.PTTGxRb+/−* mice, at ages 2, 4, 6, and 8 months. Two pituitaries from the *αGSU.PTTGxRb+/−* group (at 6 and 8 months) and 3 pituitaries from the *Rb+/−* group (1 at 4 months and 2 at 8 months) were excluded from the cohort for volume determination because they exhibited tumors. Over the study, one *αGSU.PTTG*, one *Rb+/−*, and 3 *αGSU.PTTGxRb+/−* mice died due to anesthesia-related complications. Hence, the number of pituitaries analyzed at 2, 4, 6, and 8 months was 10, 10, 9, and 9 in *αGSU.PTTG*; 9, 7, 7, and 5 in *Rb+/−*; 10, 10, 8, and 5 in *αGSU.PTTGxRb+/−*, respectively; and 8 for all ages in WT mice. Mean ± SE of the pituitary volume in pixels at 2, 4, 6, and 8 months was 179 ± 7, 200 ± 8, 199 ± 10, and 218 ± 9 in WT; 203 ± 9, 219 ± 8, 214 ± 15, and 237 ± 11 in *αGSU.PTTG*; 199 ± 7, 195 ± 9, 210 ± 12, and 221 ± 21 in *Rb+/−*; and 234 ± 12, 240 ± 17, 225 ± 11, and 241 ± 13 in *αGSU.PTTGxRb+/−* mice, respectively.

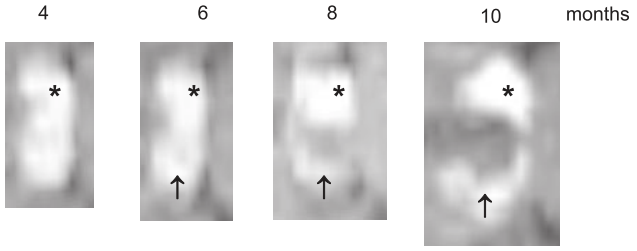

FIG. 7. Pituitary tumor onset and progression assessed by MRI. Images consist of MIP of reformatted data of pituitary gland of the same bitransgenic *αGSU.PTTGxRb+/−* mouse at 4, 6, 8, and 10 months of age. *Star* (hyperintense signal), Normal pituitary. *Arrow* (hypointense signal), pituitary tumor.

Pituitary tumor pathology

Histopathological analyses of the first pituitary tumors derived from 20 bitransgenic *αGSU.PTTGxRb+/−* and 20 *Rb+/−* mice were compared. The average age of pituitary tumor harvest was similar for both genotypes [10.7 (from 6–14) months in *αGSU.PTTGxRb+/−* mice and 10.9 (from 5–15) months in *Rb+/−* mice], and weight was also compa-

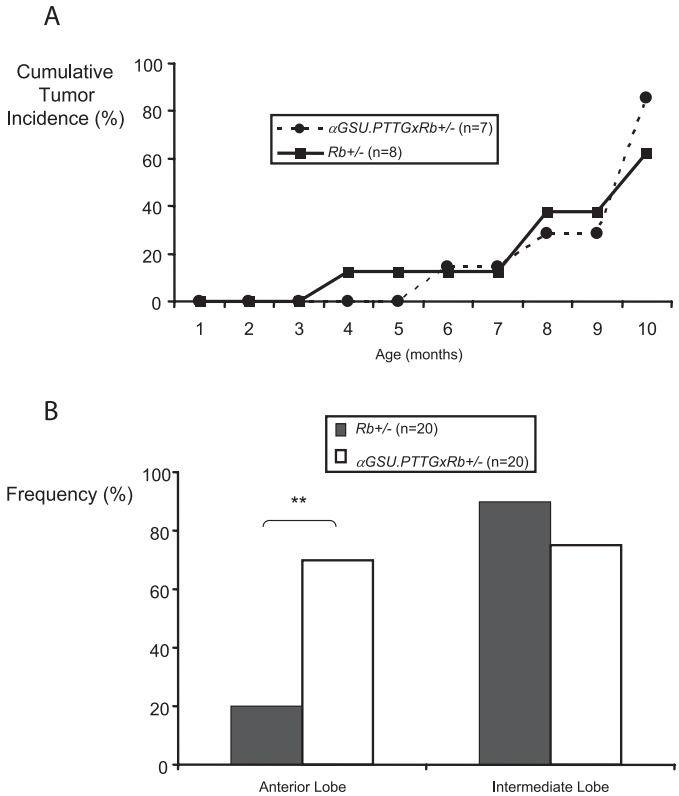

FIG. 8. Bitransgenic *αGSU.PTTGxRb+/−* mice exhibit higher prevalence of anterior lobe and similar prevalence of intermediate lobe pituitary tumors when compared with *Rb+/−* mice. A, Similar cumulative incidence of pituitary tumors in *Rb+/−* and *αGSU.PTTGxRb+/−* mice determined *in vivo* by MRI. n, Total number of animals that had pituitary gland imaged until 10 months of age or that had visible tumor in MRI. B, Pathological analysis of pituitary tumors reveals that frequency of tumors arising from anterior lobe is higher in *αGSU.PTTGxRb+/−* (*white bars*) than in *Rb+/−* (*black bars*) pituitary tumors (**, $P = 0.0036$), but frequency of tumors arising from the intermediate lobe is similar. n, Total number of pituitary tumors analyzed.

rable (mean ± SEM, 61 ± 13 mg in *αGSU.PTTGxRb+/−* and 57 ± 17 mg in *Rb+/−*). Pituitary tumors originating from the anterior lobe were distinguished from those originating from intermediate lobe by light microscopy and immunohistochemistry for pituitary hormones. Intermediate lobe tumors immunostain for ACTH only, whereas anterior lobe tumors immunostain for one or more of the anterior lobe hormones. Immunostaining profile of the pituitary tumors is listed in Table 3. Of note, in both genotypes, a subset of pituitary tumors comprised two distinct neoplasms, *i.e.* both anterior and intermediate lobe tumors coexisting in the same sample. In almost all samples, only one anterior lobe and/or one intermediate lobe tumor were observed. As indicated in Table 3, the only exception was sample 2, derived from a *Rb+/−* mouse that exhibited two distinct small anterior lobe tumors.

TABLE 3. *Rb+/−* and *αGSU.PTTGxRb+/−* pituitary tumor hormone immunostaining profile

Genotype	Sample no.	Immunohistochemistry	
		Anterior lobe	Intermediate lobe
Rb+/−			
	1	GSU	
	2	a-GSU, TSH; b-GSU, LH[a]	
	3	GH	ACTH
	4	GSU, TSH, PRL	ACTH
	5		ACTH
	6		ACTH
	7		ACTH
	8		ACTH
	9		ACTH
	10		ACTH
	11		ACTH
	12		ACTH
	13		ACTH
	14		ACTH
	15		ACTH
	16		ACTH
	17		ACTH
	18		ACTH
	19		ACTH
	20		ACTH
αGSU.PTTGxRb+/−			
	1	GH, PRL	
	2	GSU	
	3	GSU, TSH, GH, PRL	
	4	GSU,TSH	
	5	GSU,TSH	
	6	GH	ACTH
	7	GH	ACTH
	8	GSU, GH	ACTH
	9	GSU, LH, PRL	ACTH
	10	GSU, TSH, PRL	ACTH
	11	GSU,TSH	ACTH
	12	LH	ACTH
	13	TSH	ACTH
	14	GSU	ACTH
	15		ACTH
	16		ACTH
	17		ACTH
	18		ACTH
	19		ACTH
	20		ACTH

[a] Pituitary tumor sample 2 derived from an *Rb+/−* mouse exhibited two distinct anterior lobe tumors (a and b). In all other samples, only one anterior lobe and/or one intermediate lobe tumor were observed.

Eighty percent (16 of 20) of the pituitary tumors derived from *Rb+/−* mice originated from the intermediate lobe only, 10% (two of 20) from the anterior lobe only, and in two cases (10%), the pituitary exhibited tumors arising in both intermediate and anterior lobes. Thirty percent (six of 20) of pituitary tumors in *αGSU.PTTGxRb+/−* mice were of intermediate lobe origin only, 25% (five of 20) arose exclusively in the anterior lobe, and 45% (nine of 20) of pituitary tumors from bitransgenic genotype mice had adenomatous foci in both intermediate and anterior lobes. As depicted in Fig. 8B, the frequency of tumors arising from the anterior lobe was over 3.5-fold higher in bitransgenic *αGSU.PTTGxRb+/−* compared with *Rb+/−* pituitary tumors [70% (14 of 20) *vs.* 20% (four of 20), respectively; $P = 0.0036$]. The frequency of intermediate lobe tumors was similar in *αGSU.PTTGxRb+/−* and *Rb+/−* samples [75% (15 of 20) *vs.* 90% (18 of 20), respectively; $P = 0.41$].

Tumors were derived from females in 12 of the 20 *αGSU.PTTGxRb+/−* and eight of the 20 *Rb+/−* pituitary tumor samples. No sex difference in age or tumor weight was noted between genotypes. Bitransgenic *αGSU.PTTGxRb+/−* females exhibited slightly higher prevalence of anterior lobe tumors (10 of 12 tumors) compared with males with the same genotype (four of eight pituitary tumors). No sex difference in the prevalence of anterior lobe tumors was noted in *Rb+/−* mice (one of eight in females and three of 12 in males) or in the prevalence of intermediate lobe pituitary tumors in both genotypes.

To assess whether anterior lobe pituitary tumors from *αGSU.PTTGxRb+/−* and *Rb+/−* mice proliferate at different rates, we compared their PCNA staining index. The percentage of PCNA positive cells was similar in anterior lobe tumors from both genotypes (69 ± 17% *vs.* 73 ± 24% in *αGSU.PTTGxRb+/−* and *Rb+/−*, respectively) (Fig. 9).

Discussion

Pituitary trophic status may directly correlate with the likelihood of tumor development. It is, however, difficult to

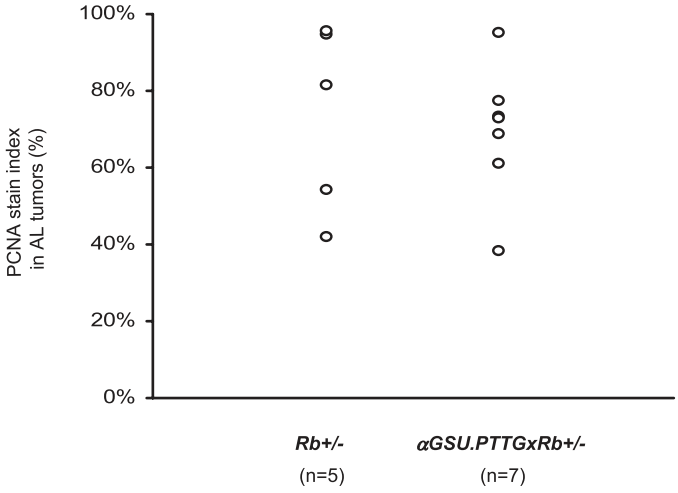

FIG. 9. Anterior lobe pituitary tumors from *αGSU.PTTGxRb+/−* and *Rb+/−* mice have similar proliferation rate. The percentage of PCNA stained cells is similar in *αGSU.PTTGxRb+/−* and *Rb+/−* anterior lobe pituitary tumors. n, Total number of pituitary tumors. AL, Anterior lobe.

test this relationship in serial human specimens. Pituitary tumors are essentially benign and occasionally are incidentally found during autopsies or imaging examinations. The prevalence of pituitary adenomas in autopsy studies ranges from 3–27% (22–26). Clinically active pituitary tumors are notably less common, with a reported prevalence of <1% (27). In a large survey including 506 patients harboring pituitary incidentalomas, the most frequent diagnosis was nonfunctioning pituitary adenoma (28). Pituitary hyperplasia or hypoplasia are not commonly reported in autopsy studies, likely due to diagnostic difficulties. Hyperplasia is defined as an abnormal increase in cell number, and may have a diffuse or nodular pattern. Morphology and anatomical distribution differs between hyperplasias of individual pituitary cell types (29). Pituitary hypoplasia, *i.e.* a small gland with decreased cell number, is infrequently encountered and usually results from genetic abnormalities linked to pituitary hormone deficiency.

Common progression of pituitary hyperplasia to neoplasia is not supported by studies of human tumor specimens. Physiological pituitary hyperplasia (pregnancy, lactation), pituitary enlargement due to estrogen administration, or untreated primary hypothyroidism are infrequently associated with adenoma development (29–32). Although true GH-secreting adenoma development in patients with ectopic GHRH syndrome has been reported (33, 34), patients harboring GHRH-producing tumors usually develop acromegaly due to somatotroph hyperplasia (34, 35). Surgically removed pituitary adenomas are often surrounded by nonhyperplastic pituitary tissue and are generally monoclonal (36, 37). However, animal models clearly show that sustained long-term pituitary hyperplasia ultimately results in tumor progression (11, 12). Whether or not sustained (several years) pituitary hyperplasia in humans results in a similarly higher incidence of neoplasia development is presently unknown. Cellular changes preceding, or not related to, gross morphological abnormalities may have a permissive effect on pituitary adenoma development.

Because PTTG abundance correlates with pituitary gland plasticity, regulation of this gene may subserve a mechanism for affecting tumor formation. *Pttg* knockout results in pituitary hypoplasia (18, 19), and *Pttg* inactivation in *Rb+/−* mice results in relative protection from tumor development (13). Although *Rb+/−* mice have a cumulative pituitary tumor incidence of 86% by 13 months, only 30% of bitransgenic *Pttg−/−Rb+/−* mice develop pituitary tumors by the same age ($P < 0.01$) (13). Targeted *PTTG* overexpression in mice driven by the αGSU promoter results in focal pituitary hyperplasia with hormone hypersecretion (19). In this study, we extend these insights, showing that combined *Rb+/−* and targeted pituitary *PTTG* overexpression enhances pituitary hyperplasia and tumor prevalence. Anterior lobe pituitary tumors arose relatively infrequently in *Rb+/−* mice, representing only 20% of tumors. Other studies on *Rb+/−* mice reported a prevalence of anterior lobe tumors ranging from 7–65%, and this variability is attributed to different genetic backgrounds (38–40). Bitransgenic *αGSU.PTTGxRb+/−* mice have enlarged pituitary glands and 3.5-fold increase in the frequency of tumors originating from α-subunit-expressing cells. A proposed depiction of effects resulting from *in vivo* changes in pituitary PTTG content is shown in Fig. 10.

PTTG overexpression permits a proliferative advantage, and this effect is enhanced by the combination with heterozygous *Rb* inactivation. By MRI analysis, we show that *αGSU.PTTGxRb+/−* mice exhibit significantly larger nontumorous pituitary glands compared with control litter mates. This enlargement was remarkable at 2 months of age, becoming less pronounced in the older age groups. When pituitary glands developed tumors, they were excluded from the cohort for volume determination, and this likely explains the attenuation of volume difference between *αGSU.PTTGxRb+/−* pituitaries and the other genotypes in the older age groups. Bitransgenic

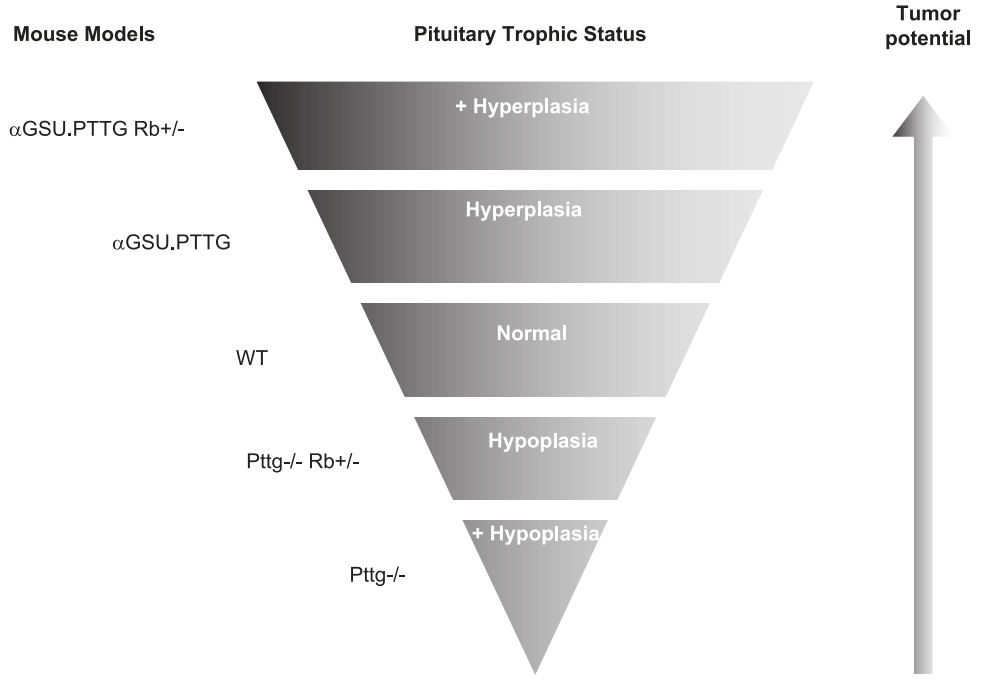

FIG. 10. Pituitary PTTG content correlates with gland plasticity and with tumor formation potential. On the *left* side of the *inverted triangle* are listed mouse models with descending pituitary PTTG content, with or without the combination with tumorigenic Rb+/−. The *horizontal bars* composing the *inverted triangle* represent the observed effects of the different genotypes on pituitary trophic status, which correlates with pituitary tumorigenic potential (*arrow*). [Modified from Ref. 55.]

αGSU.PTTGxRb+/− mice with larger pituitary glands at age 2 months were more likely to develop tumors. Pituitary volume (mean ± SEM) was 293 ± 24 in animals that developed pituitary tumors earlier than 8 months *vs.* 255 ± 18 pixels in those that developed tumors after 8 months (P = not significant). Pituitary enlargement in monotransgenic *αGSU.PTTG* and bitransgenic *αGSU.PTTGxRb+/−* mice is likely accounted for by hyperplasia of the anterior lobe, specifically of αGSU-positive cells overexpressing PTTG.

Analysis of pituitary glands by electron microscopy revealed that especially gonadotrophs, but also thyrotrophs in bitransgenic *αGSU.PTTGxRb+/−* mice, exhibit morphological changes consistent with enhanced cellular activity, such as prominent Golgi apparatus and increased secretory granule number. The ultrastructure phenotype observed in *αGSU.PTTG* gonadotrophs is consistent with LH hypersecretion previously shown in these mice that results in hypertrophy of urogenital apparatus in males (19). In agreement with the pituitary volume profile observed with MRI, morphological changes by electron microscopy were more pronounced in bitransgenic *αGSU.PTTGxRb+/−* pituitaries compared with *αGSU.PTTG* pituitaries. Cytoplasmic glycogen accumulation observed in *αGSU.PTTGxRb+/−* gonadotrophs is unusual finding in pituitary gland, and the significance of this finding is not clear.

Confocal microscopy imaging shows that pituitary cells overexpressing PTTG exhibit clear nuclear changes. Altered chromatin pattern has been described in malignant cells, ranging from coarse and irregular distribution to peripheral margination of chromatin with central clearing of the nucleus (41). A model for nuclear organization suggests that progressive cellular differentiation relates to increasingly defined transcription patterns, morphologically translating in more compact chromatin, *i.e.* smaller nuclei and more evident repressed heterochromatin. Reversal of chromatin pattern toward totipotent embryonic phenotype, where nuclei are large and there is less repressed heterochromatin, may occur during meiosis and oncogenic transformation (42). Exact causes of changes of chromatin pattern in malignancy are not known, and possible explanations are: 1) chromatin relocation due to reactivation of repressed genes; 2) qualitative and quantitative changes in nuclear matrix protein; 3) acetylation of histones, disrupting nucleosome structure that leads to DNA relaxation for increased accessibility of transcription factors; 4) DNA aneuploidy; 5) increase in nuclear pore permeability; and 6) changes in attachment of lamins (proteins lining the inner nuclear membrane) to chromatin (41). Altered chromatin pattern caused by fixation method also needs to be considered; however, this is very unlikely in our pituitary samples because of the clear differences in nuclear pattern between controls (WT pituitary and eGPF-negative cells) and eGFP-positive cells. Macronuclei and chromatin redistribution were a distinct finding in cells expressing the *αGSU-PTTG1-IRES-eGFP* transgene. Interestingly, pituitary samples analyzed under confocal microscopy were derived from young mice (2 months old) and were nontumorous. As shown above, pituitary hyperplasia is already observed at this age, particularly in *αGSU.PTTGxRb+/−* mice. Confocal microscopy images show that hyperplastic pituitaries due to PTTG overexpression exhibit chromatin pattern alteration similar to the ones reported in fully malignant cells, suggesting that PTTG overexpression results in nuclear neoplastic phenotype. Nuclear vacuolization was found in a fraction of monotransgenic *αGSU.PTTG* and bitransgenic *αGSU.PTTGxRb+/−* pituitary cells, but the significance of this finding is not clear.

Increased pituitary hyperplasia in bitransgenic *αGSU.PTTGxRb+/−* mice directly correlated with higher frequency of tumors originating from PTTG-overexpressing cells, when compared with *Rb+/−* mice pituitaries, thus supporting a permissive role of PTTG in tumorigenesis. However, tumor cell proliferation as assessed by PCNA stain index was similar in anterior lobe tumors from both genotypes. This suggests that increased PTTG content results in higher tumor penetrance, but this does not lead to more aggressive tumors. Moreover, these tumors were negative for the antiapoptotic marker bcl-2 (data not shown), indicating that tumor growth does not rely on inhibition of apoptosis.

Several proposed mechanisms may explain the role of *PTTG* on tumor development. As a securin, PTTG has the critical role of regulating sister chromatid separation during mitosis. Abnormal PTTG levels cause asymmetric sister chromatid separation and aneuploidy (17). Genomic instability has been associated with cancer (43–45) and correlates with aggressive neoplasia (46, 47), including pituitary tumors (48). However, the cause and effect relation between aneuploidy and malignant tumors remains controversial (43). In disagreement with the hypothesis that genomic instability has a causal role on tumorigenesis, it has been shown that despite causing chromosome missegregation, *Pttg* inactivation does not predispose to tumor formation (18). *Pttg−/−* mouse embryo fibroblast metaphases exhibit quadriradial, triradial, and disrupted chromosomes, as well as premature centromere division. Nevertheless, *Pttg* knockout mice demonstrate tissue-specific hypoplasia and no increase in overall tumor prevalence (18). Therefore, aneuploidy caused by abnormal *PTTG* content is likely not wholly sufficient to initiate tumor formation.

In addition to its securin function, PTTG possesses transactivation ability (49). PTTG activates c-*myc* transcription (50) and inhibits expression of the cell cycle inhibitor p21 (13). PTTG binds to the c-*myc* promoter, and this may represent a mechanism for increased cell proliferation and transformation properties (15, 50) observed in cells with high PTTG content. Changes in pituitary PTTG content also inversely correlate with p21 expression, *i.e. Pttg−/−* pituitaries exhibit increased p21 and *αGSU.PTTG* pituitaries exhibit decreased p21 levels (13). PTTG inhibits p21 promoter activity, suggesting that p21 regulation by PTTG occurs at a transcriptional level (13). Decreased levels of the cyclin-dependent kinase inhibitor p21 in *αGSU.PTTG* pituitary glands may facilitate cell cycle progression that results in focal pituitary hyperplasia. In contrast, increased p21 levels, as seen in *Pttg−/−* mice, induces interphase cell cycle arrest and is likely a mechanism contributing to pituitary hypoplasia.

Another mechanism by which PTTG may facilitate tumor formation is by inducing growth factors. PTTG induces angiogenesis, as shown with conditioned media derived from *PTTG*-transfected cells (51). The angiogenic property of PTTG is mediated by fibroblast growth factor and vascular

endothelial growth factor (51, 52), and PTTG, fibroblast growth factor, and vascular endothelial growth factor were all shown to be increased in pituitary tumors (53, 54).

Mechanisms that determine epigenetic *PTTG* regulation are currently being investigated, in particular the dynamic interaction between the *Rb1* pathway and *PTTG*. *PTTG* perturbations are likely proximal events in the cascade of pituitary cell-transforming events ranging from hyperplasia to true adenoma formation. Understanding mechanisms for controlling pituitary plasticity may ultimately result in the ability to regulate both the rate of development and progression of pituitary tumors.

Acknowledgments

We thank Dr. Run Yu for expertise in analyzing nuclear morphology and Dar-Yong Chen for performing mouse pituitary imaging.

Received April 25, 2006. Accepted June 21, 2006.

Address all correspondence and requests for reprints to: Shlomo Melmed, M.D., Cedars-Sinai Medical Center, 8700 Beverly Boulevard, Room 2015, Los Angeles, California 90048. E-mail: melmeds@cshs.org.

This work was supported by National Institutes of Health Grant CA 075979 (to S.M.) and by the Endocrine Fellows Foundation (to I.D.).

The authors have nothing to disclose.

References

1. **Farrell WE** 2005 Epigenetic mechanisms of tumorigenesis. Horm Metab Res 37:361–368
2. **Levy A, Lightman S** 2003 Molecular defects in the pathogenesis of pituitary tumours. Front Neuroendocrinol 24:94–127
3. **Musat M, Vax VV, Borboli N, Gueorguiev M, Bonner S, Korbonits M, Grossman AB** 2004 Cell cycle dysregulation in pituitary oncogenesis. Front Horm Res 32:34–62
4. **Evans CO, Young AN, Brown MR, Brat DJ, Parks JS, Neish AS, Oyesiku NM** 2001 Novel patterns of gene expression in pituitary adenomas identified by complementary deoxyribonucleic acid microarrays and quantitative reverse transcription-polymerase chain reaction. J Clin Endocrinol Metab 86:3097–3107
5. **Morris DG, Musat M, Czirjak S, Hanzely Z, Lillington DM, Korbonits M, Grossman AB** 2005 Differential gene expression in pituitary adenomas by oligonucleotide array analysis. Eur J Endocrinol 153:143–151
6. **Kim HJ, Kim MS, Park YJ, Kim SW, Park DJ, Park KS, Kim SY, Cho BY, Lee HK, Jung HW, Han DH, Lee HS, Chi JG** 2001 Prevalence of Gs α mutations in Korean patients with pituitary adenomas. J Endocrinol 168:221–226
7. **Landis CA, Harsh G, Lyons J, Davis RL, McCormick F, Bourne HR** 1990 Clinical characteristics of acromegalic patients whose pituitary tumors contain mutant Gs protein. J Clin Endocrinol Metab 71:1416–1420
8. **Spada A, Arosio M, Bochicchio D, Bazzoni N, Vallar L, Bassetti M, Faglia G** 1990 Clinical, biochemical, and morphological correlates in patients bearing growth hormone-secreting pituitary tumors with or without constitutively active adenylyl cyclase. J Clin Endocrinol Metab 71:1421–1426
9. **Spada A, Vallar L** 1992 G-protein oncogenes in acromegaly. Horm Res 38: 90–93
10. **Melmed S** 2003 Mechanisms for pituitary tumorigenesis: the plastic pituitary. J Clin Invest 112:1603–1618
11. **Asa SL, Kovacs K, Stefaneanu L, Horvath E, Billestrup N, Gonzalez-Manchon C, Vale W** 1992 Pituitary adenomas in mice transgenic for growth hormone-releasing hormone. Endocrinology 131:2083–2089
12. **Heaney AP, Horwitz GA, Wang Z, Singson R, Melmed S** 1999 Early involvement of estrogen-induced pituitary tumor transforming gene and fibroblast growth factor expression in prolactinoma pathogenesis. Nat Med 5:1317–1321
13. **Chesnokova V, Kovacs K, Castro AV, Zonis S, Melmed S** 2005 Pituitary hypoplasia in Pttg−/− mice is protective for Rb+/− pituitary tumorigenesis. Mol Endocrinol 19:2371–2379
14. **Pei XH, Bai F, Tsutsui T, Kiyokawa H, Xiong Y** 2004 Genetic evidence for functional dependency of p18Ink4c on Cdk4. Mol Cell Biol 24:6653–6664
15. **Pei L, Melmed S** 1997 Isolation and characterization of a pituitary tumor-transforming gene (PTTG). Mol Endocrinol 11:433–441
16. **Zou H, McGarry TJ, Bernal T, Kirschner MW** 1999 Identification of a vertebrate sister-chromatid separation inhibitor involved in transformation and tumorigenesis. Science 285:418–422
17. **Yu R, Lu W, Chen J, McCabe CJ, Melmed S** 2003 Overexpressed pituitary tumor-transforming gene causes aneuploidy in live human cells. Endocrinology 144:4991–4998
18. **Wang Z, Yu R, Melmed S** 2001 Mice lacking pituitary tumor transforming gene show testicular and splenic hypoplasia, thymic hyperplasia, thrombocytopenia, aberrant cell cycle progression, and premature centromere division. Mol Endocrinol 15:1870–1879
19. **Abbud RA, Takumi I, Barker EM, Ren SG, Chen DY, Wawrowsky K, Melmed S** 2005 Early multipotential pituitary focal hyperplasia in the α-subunit of glycoprotein hormone-driven pituitary tumor-transforming gene transgenic mice. Mol Endocrinol 19:1383–1391
20. **Jacks T, Fazeli A, Schmitt EM, Bronson RT, Goodell MA, Weinberg RA** 1992 Effects of an Rb mutation in the mouse. Nature 359:295–300
21. **Abramoff M** 2004 Image Processing with ImageJ. Biophotonics Int 11:36–42
22. **Siqueira MG, Guembarovski AL** 1984 Subclinical pituitary microadenomas. Surg Neurol 22:134–140
23. **Parent AD, Bebin J, Smith RR** 1981 Incidental pituitary adenomas. J Neurosurg 54:228–231
24. **Teramoto A, Hirakawa K, Sanno N, Osamura Y** 1994 Incidental pituitary lesions in 1,000 unselected autopsy specimens. Radiology 193:161–164
25. **Day PF, Guitelman M, Artese R, Fiszledjer L, Chervin A, Vitale NM, Stalldecker G, De M, V, Cornalo D, Alfieri A, Susana M, Gil M** 2004 Retrospective multicentric study of pituitary incidentalomas. Pituitary 7:145–148
26. **Molitch ME, Russell EJ** 1990 The pituitary "incidentaloma." Ann Intern Med 112:925–931
27. **Melmed S, Kleineberg D** 2003 Anterior pituitary. In: Larsen PR, Kronenberg HM, Melmed S, Polonsky KS, eds. Williams textbook of endocrinology. 10th ed. Philadelphia: Saunders; 177–280
28. **Sanno N, Oyama K, Tahara S, Teramoto A, Kato Y** 2003 A survey of pituitary incidentaloma in Japan. Eur J Endocrinol 149:123–127
29. **Horvath E, Kovacs K, Scheithauer BW** 1999 Pituitary hyperplasia. Pituitary 1:169–179
30. **Coogan PF, Baron JA, Lambe M** 1995 Parity and pituitary adenoma risk. J Natl Cancer Inst 87:1410–1411
31. **Ghannam NN, Hammami MM, Muttair Z, Bakheet SM** 1999 Primary hypothyroidism-associated TSH-secreting pituitary adenoma/hyperplasia presenting as a bleeding nasal mass and extremely elevated TSH level. J Endocrinol Invest 22:419–423
32. **Kovacs K, Stefaneanu L, Ezzat S, Smyth HS** 1994 Prolactin-producing pituitary adenoma in a male-to-female transsexual patient with protracted estrogen administration. A morphologic study. Arch Pathol Lab Med 118:562–565
33. **Shintani Y, Yoshimoto K, Horie H, Sano T, Kanesaki Y, Hosoi E, Yokogoshi Y, Bando H, Iwahana H, Kannuki S** 1995 Two different pituitary adenomas in a patient with multiple endocrine neoplasia type 1 associated with growth hormone-releasing hormone-producing pancreatic tumor: clinical and genetic features. Endocr J 42:331–340
34. **Sano T, Asa SL, Kovacs K** 1988 Growth hormone-releasing hormone-producing tumors: clinical, biochemical, and morphological manifestations. Endocr Rev 9:357–373
35. **Thorner MO, Perryman RL, Cronin MJ, Draznin MB, Johanson AJ, Rogol AD, Jane JA, Rudolf LE, Horvath E, Kovacs K, Vale W** 1982 Somatotroph hyperplasia: successful treatment of acromegaly by removal of a pancreatic islet tumor secreting a growth hormone-releasing factor. Trans Assoc Am Physicians 95:177–187
36. **Alexander JM, Biller BM, Bikkal H, Zervas NT, Arnold A, Klibanski A** 1990 Clinically nonfunctioning pituitary tumors are monoclonal in origin. J Clin Invest 86:336–340
37. **Herman V, Fagin J, Gonsky R, Kovacs K, Melmed S** 1990 Clonal origin of pituitary adenomas. J Clin Endocrinol Metab 71:1427–1433
38. **Leung SW, Wloga EH, Castro AF, Nguyen T, Bronson RT, Yamasaki L** 2004 A dynamic switch in Rb+/− mediated neuroendocrine tumorigenesis. Oncogene 23:3296–3307
39. **Nikitin AY, Juarez-Perez MI, Li S, Huang L, Lee WH** 1999 RB-mediated suppression of spontaneous multiple neuroendocrine neoplasia and lung metastases in Rb+/− mice. Proc Natl Acad Sci USA 96:3916–3921
40. **Zhou Z, Flesken-Nikitin A, Levine CG, Shmidt EN, Eng JP, Nikitina EY, Spencer DM, Nikitin AY** 2005 Suppression of melanotroph carcinogenesis leads to accelerated progression of pituitary anterior lobe tumors and medullary thyroid carcinomas in Rb+/− mice. Cancer Res 65:787–796
41. **Dey P** 2005 Chromatin pattern alteration in malignant cells: an enigma. Diagn Cytopathol 32:25–30
42. **Gasser SM** 2002 Visualizing chromatin dynamics in interphase nuclei. Science 296:1412–1416
43. **Dey P** 2004 Aneuploidy and malignancy: an unsolved equation. J Clin Pathol 57:1245–1249
44. **Draviam VM, Xie S, Sorger PK** 2004 Chromosome segregation and genomic stability. Curr Opin Genet Dev 14:120–125
45. **Rajagopalan H, Lengauer C** 2004 Aneuploidy and cancer. Nature 432:338–341
46. **Lanza G, Gafa R, Santini A, Maestri I, Dubini A, Gilli G, Cavazzini L** 1998 Prognostic significance of DNA ploidy in patients with stage II and stage III colon carcinoma: a prospective flow cytometric study. Cancer 82:49–59
47. **Salud A, Porcel JM, Raikundalia B, Camplejohn RS, Taub NA** 1999 Prog-

nostic significance of DNA ploidy, S-phase fraction, and P-glycoprotein expression in colorectal cancer. J Surg Oncol 72:167–174
48. **Bates AS, Farrell WE, Bicknell EJ, McNicol AM, Talbot AJ, Broome JC, Perrett CW, Thakker RV, Clayton RN** 1997 Allelic deletion in pituitary adenomas reflects aggressive biological activity and has potential value as a prognostic marker. J Clin Endocrinol Metab 82:818–824
49. **Wang Z, Melmed S** 2000 Pituitary tumor transforming gene (PTTG) transforming and transactivation activity. J Biol Chem 275:7459–7461
50. **Pei L** 2001 Identification of c-myc as a down-stream target for pituitary tumor-transforming gene. J Biol Chem 276:8484–8491
51. **Ishikawa H, Heaney AP, Yu R, Horwitz GA, Melmed S** 2001 Human pituitary tumor-transforming gene induces angiogenesis. J Clin Endocrinol Metab 86: 867–874
52. **Zhang X, Horwitz GA, Prezant TR, Valentini A, Nakashima M, Bronstein MD, Melmed S** 1999 Structure, expression, and function of human pituitary tumor-transforming gene (PTTG). Mol Endocrinol 13:156–166
53. **Hunter JA, Skelly RH, Aylwin SJ, Geddes JF, Evanson J, Besser GM, Monson JP, Burrin JM** 2003 The relationship between pituitary tumour transforming gene (PTTG) expression and in vitro hormone and vascular endothelial growth factor (VEGF) secretion from human pituitary adenomas. Eur J Endocrinol 148:203–211
54. **McCabe CJ, Khaira JS, Boelaert K, Heaney AP, Tannahill LA, Hussain S, Mitchell R, Olliff J, Sheppard MC, Franklyn JA, Gittoes NJ** 2003 Expression of pituitary tumour transforming gene (PTTG) and fibroblast growth factor-2 (FGF-2) in human pituitary adenomas: relationships to clinical tumour behaviour. Clin Endocrinol (Oxf) 58:141–150
55. **Donangelo I, Melmed S** 2006 Implication of pituitary tropic status on tumor development. Front Horm Res 35:1–8

***Endocrinology* is published monthly by The Endocrine Society (http://www.endo-society.org), the foremost professional society serving the endocrine community.**